uptake. Figure 3, showing CH_4 concentration against depth at Jackass Flats, indicates downward diffusion with net consumption of atmospheric CH_4 to a depth of ~2 m, coupled with upward diffusion without net consumption of a subsurface source of CH_4 to 2 m, where that CH_4 is also consumed. A similar 2-m-thick zone of atmospheric CH_4 consumption was predicted by numerical modelling of a grassland site in Illinois[24], but the thickness of such zones has not previously been verified by *in situ* measurement. This indicates that as long as a downward transport pathway is available, unfavourable conditions for methane consumption near the soil surface may allow atmospheric CH_4 to diffuse to some greater depth, where consumption can proceed under more favourable conditions. It also partly explains the inconsistent success of attempts to relate CH_4 uptake rate to soil moisture and/or temperature at a fixed depth near the surface. Precise measurements of subsurface change in CH_4 concentration and isotopic composition occurring in response to change in temperature, moisture, nutrient and physical conditions of soil are needed for better characterization of the gross CH_4 budget of all soil systems.

Our measurements indicate that desert soils are significant contributors to the global CH_4 soil sink term. They also suggest that the magnitude of CH_4 consumption by desert soils could increase substantially if there is a net increase in arid region soil moisture. Current general circulation models are, however, not capable of predicting with certainty any such regional increases (or decreases) in soil moisture in response to the various global climate change scenarios[26]. □

Received 9 January; accepted 3 April 1992.

1. Khalil, M. A. K. & Rasmussen, R. A. *Atmos. Envir.* **21,** 2445–2452 (1987).
2. Blake, D. R. & Rowland, F. S. *Science* **239,** 1129–1131 (1988).
3. Khalil, M. A. K. & Rasmussen, R. A. *Envir. Sci. Technol.* **24,** 549–553 (1990).
4. Wuebbles, D. J. & Edmonds, J. *Primer on Greenhouse Gases* (Lewis, Chelsea, Michigan, 1991).
5. Cicerone, R. J. & Oremland, R. S. *Global biogeochem. Cycles* **2,** 299–327 (1988).
6. Born, M., Dorr, H. & Levin, I. *Tellus* B**42,** 2–8 (1990).
7. Harriss, R. C. & Sebacher, D. I. *Nature* **297,** 673–674 (1982).
8. Keller, M., Goreau, T. J., Wofsy, S. C., Kaplan, W. A. & McElroy, M. B. *Geophys. Res. Lett.* **10,** 1156–1159 (1983).
9. Seiler, W., Conrad, R. & Scharffe, D. *J. atmos. Chem.* **1,** 171–186 (1984).
10. Megraw, S. R. & Knowles, R. *Biol. Fertil. Soils* **5,** 56–60 (1987).
11. Seiler, W. & Conrad, R. in *The Geophysiology of Amazonia: Vegetation and Climate Interactions* (ed. Dickinson, R. E.) 133–162 (Wiley, New York, 1987).
12. Steudler, P. A., Bowden, R. D., Melillo, J. M. & Aber, J. D. *Nature* **341,** 314–316 (1989).
13. Keller, M., Mitre, M. E. & Stallard, R. F. *Global biogeochem. Cycles* **4,** 21–27 (1990).
14. Whalen, S. C. & Reeburgh, W. S. *Nature* **346,** 160–162 (1990).
15. Yavitt, J. B., Downey, D. M., Lang, G. E. & Sexstone, A. J. *Biogeochemistry* **9,** 39–52 (1990).
16. Crill, P. M., *Global biogeochem. Cycles* **5,** 319–334 (1991).
17. Delmas, R. A., Marenco, A., Tathy, J. P., Cros, B. & Baudet, J. G. R. *J. geophys Res.* **96,** 7287–7299 (1991).
18. Mosier, A., Schimel, D., Valentine, D., Bronson, K. & Parton, W. *Nature* **350,** 330–332 (1991).
19. Whalen, S. C., Reeburgh, W. S. & Kizer, K. S., *Global biogeochem. Cycles* **5,** 261–273 (1991).
20. Whalen, S. C., Reeburgh, W. S. & Sandbeck, K. A. *Appl. envir. Microbiol.* **56,** 3405–3411 (1990).
21. Beatley, J. C. *Vascular Plants of the Nevada Test Site and Central-Southern Nevada* TID-26881 (National Technical Information Service, U.S. Department of Commerce, Springfield, 1976).
22. Hutchinson, G. L. & Mosier, A. R. *Soil. Soc. Am. J.* **45,** 311–316 (1981).
23. Whalen, S. C. & Reeburgh, W. S. *Global biogeochem. Cycles* **2,** 399–409 (1988).
24. Striegl, R. G. & Ishii, A. L. *J. Hydrol.* **111,** 133–143 (1989).
25. National Weather Service, Nevada Test Site Climatological Network (NOAA, Las Vegas, 1989–91).
26. Grotch, S. L. & MacCracken, M. C. *J. Clim.* **4,** 286–303 (1991).

Response of alluvial systems to fire and climate change in Yellowstone National Park

Grant A. Meyer*, Stephen G. Wells†, Robert C. Balling Jr‡ & A. J. Timothy Jull§

* Department of Geology, University of New Mexico, Albuquerque, New Mexico 87131, USA
† Department of Earth Sciences, University of California-Riverside, Riverside, California 92521, USA
‡ Office of Climatology, Arizona State University, Tempe, Arizona 85287, USA
§ National Science Foundation-Arizona Accelerator Facility for Isotope Dating, Building 81, University of Arizona, Tucson, Arizona 85721, USA

PROJECTIONS of the ecological effects of global climate change often include increased frequency and/or intensity of forest fires in regions of warmer and drier climate[1–3]. In addition to disturbing biological systems, widespread intense fires may influence the evolution of the physical landscape through greatly enhanced sediment transport[4]. Debris-flow to flood-streamflow sedimentation events following the 1988 fires in the Yellowstone National Park area (Wyoming and Montana, USA) have allowed us to examine the geomorphological response to fire in a mountain environment. Abundant analogous deposits in older alluvial fan sequences bear witness to past fire-related sedimentation events in northeastern Yellowstone, and radiocarbon dating of these events yields a detailed chronology of fire-related sedimentation for the past 3,500 years. We find that alluvial fans aggrade during periods of frequent fire-related sedimentation events, and we interpret these periods as subject to drought or high climatic variability. During wetter periods, sediment is removed from alluvial fan storage and transported down axial streams, resulting in floodplain aggradation. The dominant alluvial activity is strongly modulated by climate, with fire acting as a drought-actuated catalyst for sediment transport.

Fire regimes in the high-elevation conifer forests of the Yellowstone region are characterized by large, infrequent, stand-replacing events, as exemplified by the fires of 1988 (ref. 5). We have studied the effects of such fires on the northeastern Yellowstone landscape (Fig. 1*a*), an area of steep-walled glacial trough valleys cut in highly erodible Eocene volcaniclastic rocks. Small tributary basins, many with ephemeral streams, feed postglacial (paraglacial[6]) alluvial fans along the base of main valley sideslopes. In burned basins, loss of vegetative cover and addition of combustion residues to soil surfaces result in large increases in storm runoff as overland flow[4,7]. Beginning in summer 1989, charcoal-rich debris flows have been generated by brief, intense convective-storm precipitation in small, steep, intensely burned basins with little postfire regrowth. Fine sediment, ash and charcoal entrained by sheetwash and rilling of burned soil surfaces combine with coarser sediment derived from channel incision to produce the high sediment concentration of these flows. Larger basins tend to produce more-dilute newtonian-flood streamflows, and hyperconcentrated flows (transitional from streamflow to debris flow)[8,9]. Runoff from a single storm commonly progresses towards more dilute flow but may also be dominated by a single process. Since 1989, events have been less frequent, mostly because of revegetation, and more dilute, probably because of processes that decrease fine sediment availability even on unvegetated slopes[10]. Instability persists, however, because deep incision accelerates ravelling and slumping into channels of event basins.

We examined deposits produced by a range of post-1988 fire-related sedimentation processes to develop models for identification of similar deposits within alluvial fan sequences in northeastern Yellowstone. In debris flows, large clasts settled and were emplaced in bouldery lobes where flows became unconfined below the alluvial fan apex. Fines-dominated runout slurries continued downfan, depositing thin, widespread lobes of very poorly sorted muddy sand with abundant charcoal and organic material (Fig. 1*b*). Similar charcoal-rich debris-flow deposits are common in northeastern Yellowstone fan sequences, and provide diagnostic records of fire-related sedimentation which can be radiocarbon-dated.

Charcoal remains suspended in more-dilute flows and is therefore rare within fire-related hyperconcentrated-flow and streamflow fan deposits. Many alluvial fan stratigraphic sections in

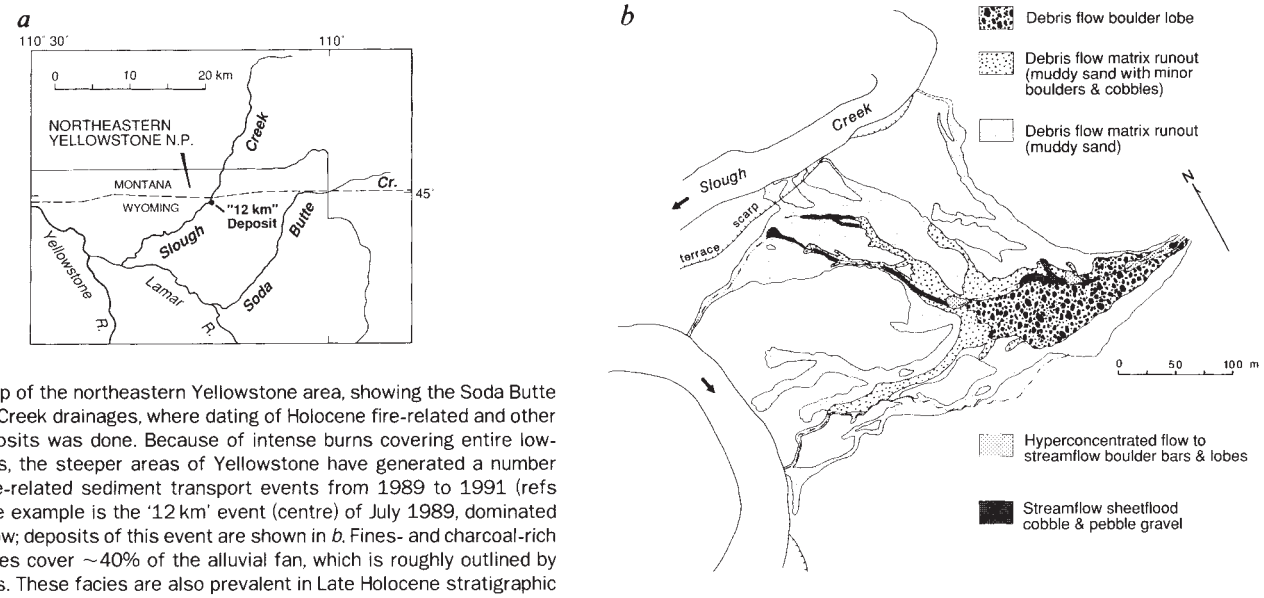

FIG. 1 *a*, Map of the northeastern Yellowstone area, showing the Soda Butte and Slough Creek drainages, where dating of Holocene fire-related and other alluvial deposits was done. Because of intense burns covering entire low-order basins, the steeper areas of Yellowstone have generated a number of large fire-related sediment transport events from 1989 to 1991 (refs 28, 29). One example is the '12 km' event (centre) of July 1989, dominated by debris flow; deposits of this event are shown in *b*. Fines- and charcoal-rich run-out facies cover ~40% of the alluvial fan, which is roughly outlined by the deposits. These facies are also prevalent in Late Holocene stratigraphic sections of alluvial fans.

Yellowstone, however, contain thin, burned-in-place soil surface layers. Preservation of these charcoal-rich layers without bioturbation requires rapid burial; post-1988 fire-related sediments have buried an intact 1988 burned surface in several localities. Using this analogue, we interpret hyperconcentrated-flow and streamflow facies units directly overlying well preserved burned-in-place layers as probable fire-related deposits (less confidently interpreted as fire-related than are charcoal-rich debris-flow deposits). Data from 25 stratigraphic sections in northeastern Yellowstone show that fire-related debris-flow and probable fire-related sediments make up ~30% of the volume of late Holocene alluvial fan materials. A substantial part of the remaining volume is likely to be reworked or nondiagnostic fire-related sediment. Fire has been an important factor in sediment transport from slopes and low-order channels into storage on alluvial fans.

We identified and radiocarbon-dated 18 fire-related debris-flow events and 17 probable fire-related sedimentation events spanning the past 3,500 years in the Soda Butte and Slough Creek drainages of northeastern Yellowstone (Figs 1 and 2). Data on earlier Holocene events (not shown) are relatively sparse because of limited exposure. Tree-ring calibrated[11] ages are plotted in the histogram in Fig. 2; where multiple calibrated ages are possible for one radiocarbon date, the date is plotted in the interval containing the greatest area underneath the calibrated probability density distribution (CPDD) for that date. The normal distribution defined by the ^{14}C date and its analytical standard deviation is transformed to a CPDD through the calibration curve in the computer program CALIB[11]. Probability density curves in Fig. 2 are constructed by summing individual CPDDs for the same 35 dates shown in the histogram, where each date contributes an equal portion of the area under the curve. The highest frequency of variation in the curve largely represents multiple possible calibrated ages for single events (compare histogram and curve). The curve is truncated at AD 1872 because historical records and stratigraphic relations constrain the youngest fire-related event to before that date. The peak near AD 1700 probably represents the last widespread fires in Yellowstone, as recognized in ~350-yr dendrochronological[5,12] and lake sediment[13] fire histories.

Although most dated samples from fire-related sediments were aggregates of charcoal fragments, we obtained five dates on individual charcoal fragments from one debris-flow unit (Fig. 2). Distributions for four of these dates strongly overlap, implying that aggregate sample dates primarily reflect one age of charcoal: that from the associated fire.

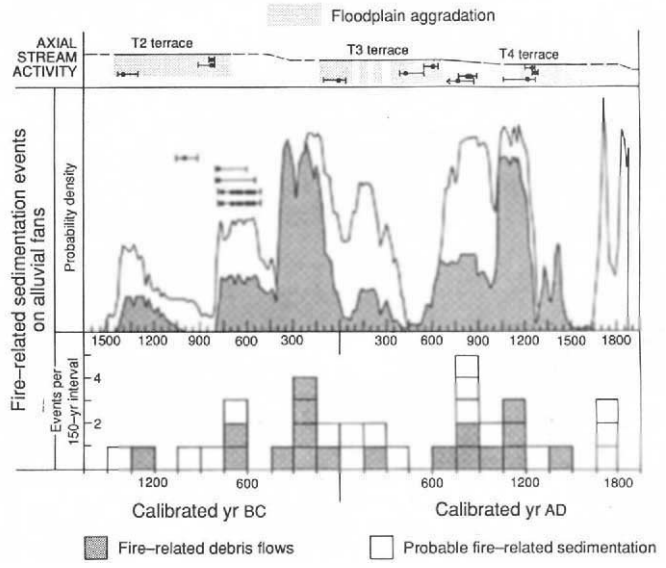

FIG. 2 Summary of fire-related sedimentation and other alluvial activity in the Soda Butte and Slough Creek drainages for the past 3,500 years. Histogram and probability density curves show the distribution of calibrated ^{14}C dates[11] (in calendar years) on 35 independent events interpreted as either fire-related debris flows or probable fire-related sedimentation events (see text). Solid circles and error bars above the left end of the curve depict calibrated age(s) and 1σ calibrated age ranges for five dated charcoal fragments from a single fire-related debris-flow unit; only the youngest date is included in the curve. Top of diagram shows time of activity on the T2, T3 and T4 axial stream terraces, including floodplain aggradation (patterned bars) and downcutting between levels (sloping lines), as constrained by associated calibrated ^{14}C dates (solid circles and error bars). Symbols are dashed where activity is uncertain. Date with arrow on error bar (←) denotes a minimum limiting age for T3 floodplain aggradation, and date directly above represents a local time of downcutting to T4 level.

Fire-related alluvial fan sedimentation events show strong clustering within the intervals of 800 BC–AD 350 and AD 650–1250, and sediment accumulation rates indicate concurrent rapid aggradation of the northeastern Yellowstone fans. Records of non-arboreal pollen[14] and the relative abundance of xeric- and mesic-adapted small mammals[15] in northern Yellowstone indicate that effectively drier summer conditions prevailed over these intervals. Maxima of fire-related debris-flow activity occur around 350–100 BC and AD 1000–1200 (Fig. 2); the latter maximum occurs within the widely recognized Mediaeval Warm Period (~AD 900–1300[16] with optimum at ~AD 1090–1230[17,18]). It thus seems that fire-related sedimentation is most active during centennial-scale drought-dominated periods (Fig. 3*b*).

Our analyses of historical records (1895–1989) of climate and fires in Yellowstone show that 36% of the temporal variance in annual burn area is explained by drought-related surface climate variables for the concurrent summer and preceding winter[19]. Because large fires may occur with short, severe drought (1–2 yr), and subsequent intense precipitation is also required to mobilize sediment, an alternative (but not exclusive) hypothesis is that fire-related sedimentation is generated by high short-term climate variability. The relatively low precision of ^{14}C ages makes this possibility difficult to evaluate. Coincidentally, evidence for high decadal to interannual variability combined with anomalous warmth is seen in tree-ring series from the western United States[20,21] and Fennoscandia[22] around AD 1160, corresponding roughly with a major peak in fire-related debris-flow activity in northeastern Yellowstone (Fig. 2).

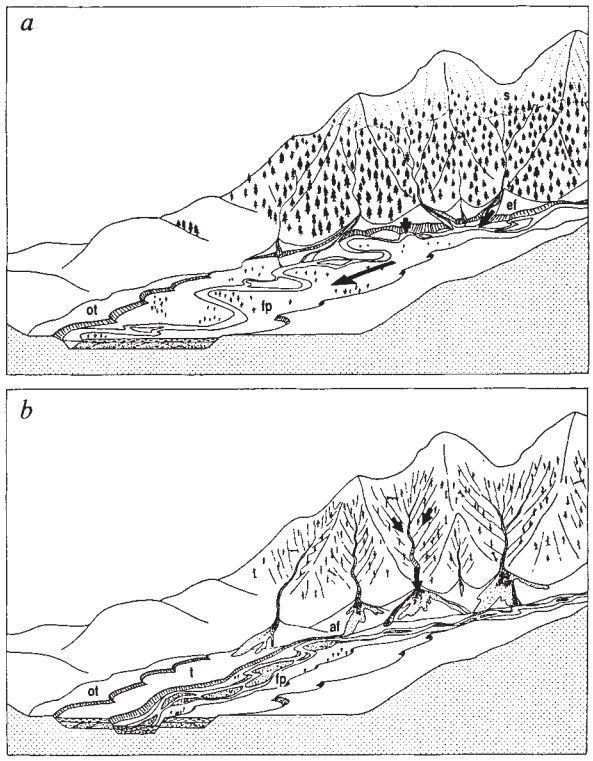

FIG. 3 Sketches of idealized Holocene alluvial activity modelled after Soda Butte Creek, with arrows denoting dominant modes of sediment transport; exaggerated for clarity. *a*, Activity during wetter periods, characterized by high snowmelt runoff (s), erosion of alluvial fans (ef) by fan channel incision and fan toe undercutting, and floodplain (fp) widening and aggradation along the lower axial stream, where sideslope sediment input is low. An older terrace (ot) remains from a previous period of floodplain aggradation. *b*, Activity during drier periods, with recently burned slopes supplying abundant sediment for debris-flow transport to aggrading alluvial fans (af). The axial stream is incising within a narrow active floodplain (fp), leaving the former wet-phase floodplain of *a* as a terrace (t).

We obtained calibrated ^{14}C dates on Soda Butte and Slough Creek axial stream sediments, from a variety of stratigraphic settings and sample types (Fig. 2). Although the late Holocene trend in lower Soda Butte Creek has been one of downcutting, this trend has been interrupted by periods of floodplain widening and aggradation which are recorded in terrace deposits. Each of these periods corresponds to a minimum of fire-related fan sedimentation. Floodplain deposits of the T3 and T4 terraces began aggrading shortly after major episodes of fire-related sedimentation, probably as these sediment loads reached downstream locations[23]. The relatively low fire-related activity preceding T2 floodplain aggradation, however, implies that fluctuations in hydroclimate and annual snowmelt runoff (which produces most of the water and suspended sediment discharge in these streams at present[24]) may more effectively control axial stream activity than slope-derived sediment supply. Local palaeoenvironmental data[14,15] characterize periods of floodplain aggradation as effectively wetter, particularly the T3 floodplain aggradation period culminating around AD 350–650 (Fig. 2). In this same period, we have also found evidence for large-scale slumping of previously stable Pleistocene deposits, greatly increased activity of a travertine-depositing spring and an increase in channel sinuosity in lower Soda Butte Creek. These changes are consistent with higher groundwater levels and increased frequency of small overbank floods. Sharply declining fire-related sedimentation and early T4 floodplain construction following AD 1200 are coincident with onset of the Little Ice Age elsewhere in North America[18,21,25]. Although a large pulse of fire-related sedimentation precedes this period, floodplain widening and aggradation of the T4 terrace is relatively minor, and is more consistent with the slight increase in effective precipitation due to cooling implied by local palaeoenvironmental data[14,15]. With increased average stream power in wetter periods, the dominant alluvial activity switches to removal of sediment from alluvial fan storage and downstream transport. Increased sediment discharge causes temporary reversal of the downcutting trend in lower reaches of axial streams, and floodplain aggradation results (Fig. 3*a*).

Low-amplitude climate changes were sufficient to induce considerable adjustments in these alluvial systems. Despite regional variations in the nature of late Holocene climate change and resultant geomorphological response, the timing of alluvial episodes in northeastern Yellowstone is similar to that in other parts of the western United States[26]. More gradual response to climate variations may occur through vegetation change in the absence of fire, but late Holocene changes in forest/grassland ratio and vegetation density occurred mainly at lower elevations in Yellowstone[14,27]. Such changes probably had limited effects on high-elevation alluvial systems[26], and were subordinate to the major slope erosion and fan deposition caused by short-term severe drought and temporary, total devegetation by fire. □

Received 21 November 1991; accepted 25 March 1992.

1. Clark, J. S. *Nature* **334,** 233–235 (1988).
2. Overpeck, J. T., Rind, D. & Goldberg, R. *Nature* **343,** 51–53 (1990).
3. Romme, W. H. & Turner, M. G. *Conserv. Biol.* **5,** 373–386 (1991).
4. Swanson, F. J. in *Fire and Ecosystem Processes, USDA-Forest Service General Tech. Rep.* WO-26 (eds Mooney, H. A., Bonnicksen, T. M., Christensen, N. L., Lotan, J. E. & Reiners, W. A.) 401–420 (1981).
5. Romme, W. H. & Despain, D. G. *Bioscience* **39,** 695–699 (1989).
6. Ryder, J. M. *Can. J. Earth Sci.* **8,** 279–298 (1971).
7. Wells, W. G. II in *Debris Flows/Avalanches* (eds Costa, J. E. & Wieczorek, G. F.) 105–114 (*Geological Society of America*, Boulder, 1987).
8. Pierson, T. C. & Costa, J. E. in *Debris Flows/Avalanches* (eds Costa, J. E. & Wieczorek, G. F.) 1–12 (*Geological Society of America*, Boulder, 1987).
9. Wells, S. G. & Harvey, A. M. *Bull. geol. Soc. Am.* **98,** 182–198 (1987).
10. Collins, B. D. & Dunne, T. *Earth Surface Processes and Landforms* **13,** 193–205 (1988).
11. Stuiver, M. & Reimer, P. J. *Users Guide to the Programs CALIB & DISPLAY 2.1* (Quaternary Isotope Lab., Univ. of Washington, 1987).
12. Barrett, S. W. & Arno, S. F. in *Univ. of Wyoming-Nat. Park Service Research Center 14th Annual Rep.* (eds Boyce, M. S. & Plumb, G. E.) 131–133 (UW-NPS Research Center, Laramie, 1990).
13. Millspaugh, S. H. thesis, Univ. of Pittsburgh (1991).
14. Gennett, J. A. thesis, Univ. of Iowa (1977).
15. Barnosky, E. A. *Historical Biology* (in the press).
16. Lamb, H. H. *Climate*, Vol. 2 (Methuen, London, 1977).
17. Williams, L. D. & Wigley, T. M. L. *Quat. Res.* **20,** 286–307 (1983).

18. Porter, S. C. *Quat. Res.* **26,** 27–48 (1986).
19. Balling, R. C. Jr, Meyer, G. A. & Wells, S. G. *Clim. Change* (in the press).
20. LaMarche, V. C. Jr *Science* **183,** 1043–1048 (1974).
21. LaMarche, V. C. Jr & Stockton, C. W. *Tree-Ring Bull.* **34,** 21–45 (1974).
22. Briffa, K. R. *et al. Nature* **346,** 434–439 (1990).
23. Laird, J. R. & Harvey, M. D. in *Drainage Basin Sediment Delivery* (ed. Hadley, R. F.) 165–183 (*International Association of Hydrological Sciences*, Wallingford, 1986).
24. Ewing, R. & Mohrman, J. in *Symp. Proc. Headwaters Hydrology* (eds Woessner, W. W. & Potts, D. F.) 213–222 (American Water Resources Association, Bethesda, Maryland, 1989).
25. Osborn, G. & Luckman, B. H. *Quat. Sci. Rev.* **7,** 115–128 (1988).
26. Knox, J. C. in *Late-Quaternary Environments of the United States*, Vol. 2 (ed. Wright, H. E. Jr) 26–41 (Univ. of Minnesota Press, Minneapolis, 1983).
27. Baker, R. G. in *Late-Quaternary Environments of the United States*, Vol. 2 (ed. Wright, H. E. Jr) 109–127 (Univ. of Minnesota Press, Minneapolis, 1983).
28. Meyer, G. A. & Wells, S. G. *Geol. Soc. Am. Abstr. Progr.* **23(4),** 48 (1991).
29. Johansen, E. A. *Geol. Soc. Am. Abstr. Progr.* **23(5),** A121 (1991).

ACKNOWLEDGEMENTS. We thank K. Pierce for insights on Yellowstone geomorphology; R. Mason, C. Inoue, D. Katzman and J. Rogers for field assistance; P. Reimer for help with radiocarbon calibration; and the US National Park Service–Yellowstone and US Forest Service for cooperation. Funding was provided by the National Science Foundation (S.G.W., P.I. and to NSF–Arizona Accelerator Facility), the Geological Society of America (Research and Mackin Grants) and Sigma Xi.

Reactivation of an oceanic fracture by the Macquarie Ridge earthquake of 1989

Shamita Das

Department of Earth Sciences, University of Oxford, Parks Road, Oxford OX1 3PR, UK

THEORETICAL calculations show[1] that the occurrence of an earthquake leads to regions of increased shear stress on both sides of the ruptured fault. If this stress increase is sufficiently large, or if neighbouring faults are close to their failure stress, the result may be triggering of earthquakes on pre-existing faults in the region. A search for this effect[2] produced only a few examples, all in continental areas, where clusters of aftershocks were located in the regions of increased stress. The linear dimensions of these clusters were generally less than 20 km, and less than one-half of the fault length that ruptured in the main shock. Here I report an example of this phenomenon in which the fault that is reactivated is a nearly 175-km-long segment of an oceanic fracture, and its length is comparable to that of the main shock, the 1989 Macquarie Ridge earthquake.

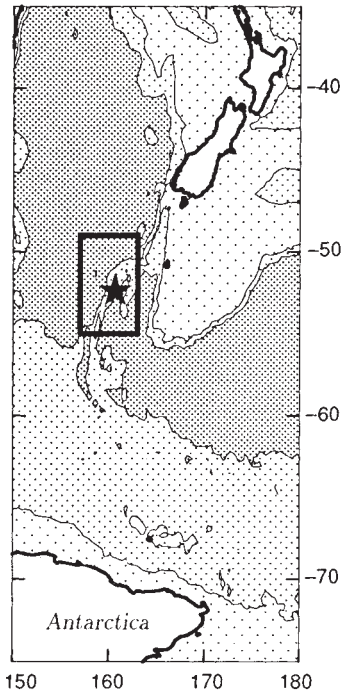

FIG. 1 Map of the Macquarie Ridge area. Bathymetric contours are shown at depths of 2,000, 4,000 and 6,000 m with the darker shading indicating deeper regions. The star denotes the epicentre of the 23 May, 1989 Macquarie Ridge earthquake. The Macquarie Ridge complex extends roughly north–south between South Island, New Zealand and the Pacific–Antarctica spreading centre. The box indicates the area shown in detail in Figs 2–4.

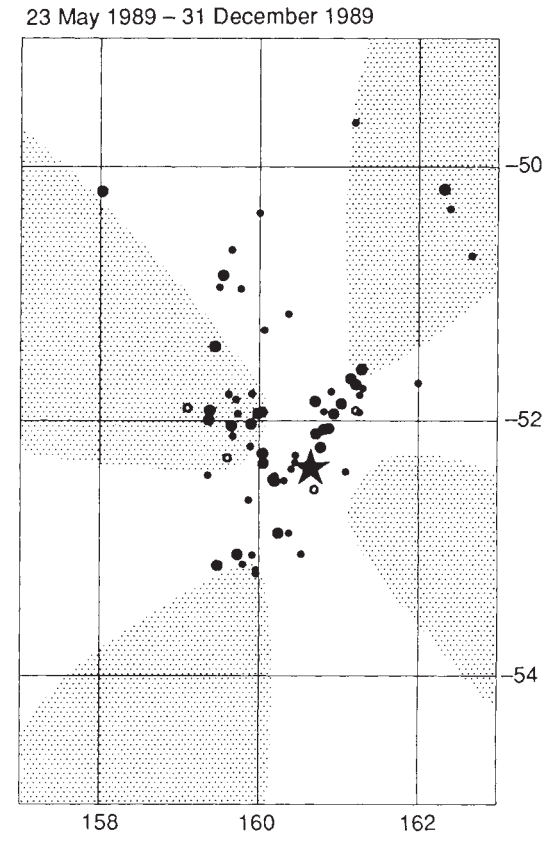

FIG. 2 *a*, Relocated aftershock epicentres for all events within the box in Fig. 1 during the period from 23 May 1989 to 31 December 1989, indicated by solid circles. The Macquarie Ridge main shock is plotted as a star. Larger symbol sizes indicate larger events. The 79 aftershocks had magnitudes in the range given by $3.8 \leq m_b \leq 5.6$, with 10 of them being too small for ISC to be able to assign a magnitude to them. These events are indicated by open circles (one size). Aftershocks are seen to concentrate on two linear zones, one being the India/Australia–Pacific plate boundary and the other being an elongated feature to its west. Events with $m_b \geq 5.0$ generally have location errors of less than a few kilometres, with the error decreasing with increasing earthquake magnitude. The four small aftershocks to the east of the Macquarie Ridge have large errors of location in the east–west

The 23 May 1989 Macquarie Ridge earthquake ($M_w = 8.2$), with a seismic moment 1.34×10^{21} N m (ref. 3), was the largest seismic event to have occurred globally for ~12 years and the largest on the India/Australia–Pacific plate boundary south of New Zealand in more than 70 years (Fig. 1). The main shock has been the subject of several studies[4,5]. From readings of arrival times at worldwide stations compiled by the International Seismological Centre (ISC), all events near this earthquake for which at least seven stations reported *P*-wave readings between 1 January 1964 and 31 December 1989 were relocated using the method of joint hypocentre determination (JHD89)[6]. Figure 2*a* shows the aftershock distribution and Fig. 2*b* the seismicity from 1964 until the day before the main shock. Figure 3*a* shows the aftershocks with their Harvard centroid moment tensor (CMT) solutions [7,8] superimposed on the bathymetry, and Fig. 3*b* the same for the 25-year period preceding the event (from quarterly listings[9] of CMT solutions since 1977).

The aftershock map shows that there are two linear zones along which the aftershocks are concentrated. One is a 220-km segment of the India/Australia–Pacific plate boundary on which the main shock occurred[3–5]. The other is a linear feature to its